EUROPEAN FUSION DEVELOPMENT AGREEMENT

EFDA–JET–PR(01)120

L.Zabeo et al

A Versatile Method for the Real Time Determination of the Safety Factor and Density Profiles in JET

A Versatile Method for the Real Time Determination of the Safety Factor and Density Profiles in JET

L.Zabeo[1] , A.Murari[1], E.Joffrin[2], D.Mazon[2], C.Taliercio[1]

[1]Consorzio-RFX Associazione ENEA-Euratom per la Fusione, C.so Stati Uniti 4, 30127 Padova, Italy

[2]Association Euratom-CEA pour la Fusion, CEA Cadarache, F-13108 Saint Paul-lez-Durance, Cedex, France

Paper submitted for publication in PPCF

ABSTRACT

In this paper, the algorithms to determine the safety factor q and density profiles in real time are presented. They have been designed to be implemented in JET,in the framework of the real time enhancements for the control of the Internal Transport Barriers (ITB). In this method, only the signals of the magnetic diagnostics and of the interferometer polarimeter are used. Instead of solving the equilibrium equation, which at the moment does not seem fully compatible with real time requirements, the topology of the magnetic surfaces is determined on the basis of the external magnetic measurements. Then the density and poloidal field profiles are found inverting the interferometric and polarimetric measurements respectively. Once the poloidal field has been obtained, the q profile is inferred. The density profiles obtained have been checked against the JET LIDAR diagnostic, showing very good agreement. On the other hand, the q profiles have been compared with the results of several versions of the equilibrium code EFIT, proving that the algorithms developed can identify with good precision both monotonic and reversed shear profiles. An optimised version of the code has also been written and it has been verified that the computing time is compatible with the requirements of JET real time system. The present algorithm is being implemented and is going to be used during JET experimental campaigns.

1. INTRODUCTION

Even if the reference scenario for a Tokamak fusion reactor is still the ELMy H-mode, characterised by a strong transport barrier at the edge, considerable many effort have been devoted in recent years to improving also the transport in the plasma core. Regimes with enhanced performance, due to a reduced thermal transport in the central region, have been identified in all major tokamaks such as JET [1], TFTR [2] and DIII [3]. In general the better performance is due to the presence of one or more internal transport barriers (ITB), which are characterised by an improved confinement region in the plasma core. Although the detailed mechanisms responsible for the reduction of the transport are not completely understood yet, it has been demonstrated that the current profile plays a leading role in their formation [4]. In particular in JET, a reversed or slightly positive q profile appears to be an indispensable ingredient. The very interesting prospects of ITBs have motivated the development of optimised methods of feedback control. In this perspective, the real time determination of the q and density profiles are of crucial importance, due to the role that these plasma parameters play in the formation and sustainement of the barriers. In this paper some algorithms to determine these two profiles are reviewed in detail. The methods adopted are based on magnetic measurements and infrared polari-inteferometer, whose signals will be available in real time in JET. Moreover, it was necessary to find a procedure, which does not solve the entire equilibrium equations, because this alternative was considered too demanding in terms of computational time. Indeed, high time resolution is an important requirement in the feedback control of ITB. The main characteristics of the procedure

adopted to determine the density and q profiles is summarised in the following. The magnetic topology is first derived (see section 2) using the magnetic measurements, from which the shape and position of the last closed magnetic flux surface and the radial dependence of the relevant shape parameters (like elongation and triangularity) are determined. This approach gives satisfactory results in practically of the entire plasma volume.

Once the magnetic surfaces have been determined, the measurements of the interferometer (Ni = line integral of the density along chord i), whose lines of sight are illustrated in fig.1, can be inverted to infer the density profile (see section 3).

The density profile is a prerequisite to the derivation of the poloidal field from the polarimetric data, which are taken along the same lines of sight as the interferometer (see section 4). The Faraday rotation angle, measured by the polarimeter, is proportional to the product of the density and the poloidal field along the line of sight according to:

$$\Delta\Gamma = C\lambda^2 \int_l n_e(l) B_{ll}(l) dl \qquad (1)$$

where n_e is the density, B_{ll} the component of poloidal magnetic field parallel to the propagation direction of the laser beam, C is a dimensional constant ($C = 2{:}615 \times 10^{-13}\ T^{-1}$), λ is the laser wavelenght ($\lambda = 194{:}7\mu m$) and the integral is taken along the line of sight *l*. The inversion procedure of these integral measurements provides the poloidal flux derivative in fuction of minor radius ($\delta\Psi/\delta\delta\rho$) at each of the previously determined magnetic surfaces. Since the toroidal field is known, follows the q profile from the relation:

$$q = \frac{d\Phi / dV}{d\Psi / dV} \qquad (2)$$

where Φ is the toroidal flux and Ψ the poloidal flux. In sections 2, 3 and 4 the different parts of the method are described in detail and the results from an extensive test campaign on optimised shear equilibria are reported. In the section 5 the optimisation of the code and its performance in terms of economy of computational time are discussed. Future developements and conclusions are the subject of the last section.

2. MAGNETIC TOPOLOGY AND MODELLING OF THE POLOIDAL FIELD

For our application, JET magnetic surfaces can be satisfactorily expressed by the relations, [5]:

$$f(R; Z) = \begin{array}{l} R = R_{axis} + \Delta(\rho) + \rho\cos(\vartheta + \gamma(\rho)\sin\vartheta) \\ Z = Z_{axis} + \rho K(\rho)\sin\vartheta \end{array} \qquad (3)$$

where ρ is the radial co-ordinate, Raxis and Zaxis the co-ordinates of the magnetic axis, $\Delta(\rho)$ the magnetic shift, $\Delta(\rho)$ the triangularity and $K(\rho)$ expresses the elongation. Since each flux surface has a different geometrical axis, defined by $R_{axis} + \Delta(\rho)$, it is also worth mentioning that the angle theta is to be calculated in the reference frame of each surface. The last closed flux surface (LCFS) is derived from the magnetic measurements [6]. On the other hand, a systematic analysis

of equilibria calculated by the EFIT code has shown that the plasma shift, elongation and triangularity functions can be assumedto be monotonic and can be expressed by the relations:

$$\Delta(\rho) = \left(\frac{\rho}{\rho_{LCFS}}\right)^{\alpha_S} \Delta_{LCFS} \tag{4}$$

$$K(\rho) = K_{axis} = + a_2 \left(\frac{\rho}{\rho_{LCFS}}\right)^2 + a_4 \left(\frac{\rho}{\rho_{LCFS}}\right)^2 \tag{5}$$

$$\gamma(\rho) = \gamma_{LCFS} = \left(\frac{\rho}{\rho_{LCFS}}\right)^{\alpha_T} \tag{6}$$

where $\Delta_{LCFS} = R_0 - R_{axis}$, R_0 geometrical axis of last closed flux surface and Kaxis is the elongation in the core.

To complete the magnetic topology in the interior of the plasma, the constants in equations (4), (5) and (6) have to be determined. These values can be obtained from the poloidal field at the edge, measured by the pick up coils [6]. For the time being, it is important to mention that the two coefficients in relation (5) allow distinguishing an upper and lower elongation, which are bearing an important role in properly reproducing the magnetic surfaces. Also for the triangularity two different sets of parameters for the upper and lower regions of the plasma are used. The radial and vertical components of the poloidal field at the LCFS derive from the pick-up coils [6]. In general these components inside the plasma are written in function of the poloidal flux as

$$B_p^R(R, Z) = -\frac{1}{2\pi R}\frac{\delta\Psi}{\delta Z} \tag{7a}$$

$$B_p^Z(R, Z) = -\frac{1}{2\pi R}\frac{\delta\Psi}{\delta Z} \tag{7b}$$

In the $(\rho:\vartheta)$ system of coordinates, B^R_p and B^Z_p can be expressed as the product of one term depending only on the geometry (topology) of the flux surfaces and one linked directly to the poloidal flux:

$$B_p^R(R, Z) = -\frac{1}{2\pi R}\frac{\delta\Psi}{\delta Z} G^{R,Z}(\rho, \vartheta, \Delta, \Delta', \gamma, \gamma', K, K') \tag{8}$$

In (8) the prime indicates the derivative with respect to ρ. $G^{R;Z}$ are coefficients which depend only on the geometry of the magnetic surfaces, since they are the derivatives of ρ with respect to R and Z respectively. The relations (8) can indeed be written as:

$$\begin{aligned} B_p^R(\rho, \vartheta) &= -\frac{1}{2\pi R}\frac{\delta\Psi}{\delta Z}\frac{\delta\rho}{\delta Z} \\ B_p^Z(\rho, \vartheta) &= -\frac{1}{2\pi R}\frac{\delta\Psi}{\delta Z}\frac{\delta\rho}{\delta Z} \end{aligned} \tag{9a}$$

In (9a) and (9b) the derivates of ρ with respect to R and Z are obtained using a transformation of the coordinates from (R; Z) to (ρ, ϑ), with the help of the Jacobian.

To determine the radial trend of the shift, the poloidal field can be calculated from relations (2) at the horizontal plane including the magnetic axis, where the radial component is zero. At these positions (for Z = Zaxis and ϑ = 0; π) one obtains:

$$B_p(\rho_{LCFS}, \vartheta = 0) = \frac{1}{2\pi R_{(\rho_{LCFS},\, \vartheta = 0)}} \frac{\delta\Psi}{\delta\rho} \frac{1}{1+\Delta'_{LCFS}} \tag{10}$$

$$B_p(\rho_{LCFS}, \vartheta = 0) = \frac{1}{2\pi R_{(\rho_{LCFS},\, \vartheta = \pi)}} \frac{\delta\Psi}{\delta\rho} \frac{1}{1-\Delta'_{LCFS}} \tag{11}$$

Since the poloidal field at the edge is measured and available in real time, the ratio of equations (10) and (11) gives the plasma shift radial dependance Δ'_{LCFS} and therefore, from the derivative of relation (4), the α_s exponent can be determined. An analogous method is adopted for the elongation; in this case the poloidal field is evaluated at $\vartheta = \pi/2$, where the vertical component is zero. In this case the relevant equation is:

$$B_p(\rho_{LCFS}, \vartheta = \tfrac{\pi}{2}) = \frac{1}{2\pi R_{(\rho_{LCFS},\, \vartheta = \frac{\pi}{2})}} \frac{\delta\Psi}{\delta\rho} \frac{1}{K + K'_\rho} \tag{12}$$

Since the derivative of the poloidal flux at the edge is available, because it can be derived from (10) or (11), relation (12) provides the radial derivative of elongation K', which, inserted in (5), allows deriving the coefficients a2 and a4 from the following simple linear system.

$$\begin{cases} K(\rho_{LCFS}) = K_{axis} + a_2 + a_4 \\ K'(\rho_{LCFS}) = 2a_2 + 4a_4 \end{cases} \tag{13}$$

In particular for the bottom of the plasma an approximation is used. It is necessary because at $\vartheta = -\pi/2$,correspond a region close to the x-point.

A similar procedure can also be adopted for the evaluation of the radial dependance of triangularity using any different value of ϑ in (2) and Δ', K' previously calculated (in our case for ϑ the angle of 45 degrees has been adopted). Typically for the exponent α_T in (6) a value of 3 or 4 can be assumed without affecting the results of the procedure very much.

To illustrate the quality of the described method, in fig.2 the magnetic surfaces reconstructed by the equilibrium code EFIT are compared with the output of our procedure for a typical optimised shear discharge (Pulse No 51590 with 2 MA plasma current and $\beta_{pol} = 0.15$ and $\beta_{MHD} = 0.08$). The agreement is good, particularly in the external region of the plasma. In the core, the main source of error resides in the uncertainty associated with the position of the magnetic axis. Since this problem is not relevant in the determination of the density but plays an important role in the reconstruction of the q profile, the technique used to overcome this difficulty will be described in section 4.

3. DENSITY PROFILE RECONSTRUCTION

The procedure described in the previous section allows the determination of the magnetic topology, which is an essential prerequisite to the implementation of any inversion method. Once the magnetic surfaces are fixed, the line integral of the interferometer can be inverted under the assumption that the density is a flux function, i.e. does not change on a flux surface. Moreover, the density profiles relevant for our application are well described by a relation of the form:

$$n_e(\rho) = n_e(1 - \rho^2)\,(1 + n_1\rho^2 + n_2\rho^4) + n_w \tag{14}$$

The relation between the three parameters n_0, n_1 and n_2 and the experimental interferometric measurements can be cast in matrix form [A][X] = [N], where [A] is the $n_{chords} \times 4$ matrix to be inverted (which contains the geometrical constants) and [N] contains the experimental measurements. The Single Value Decomposition (SVD, [7]) has been adopted to perform the required pseudo inversion. Since the H mode configuration quite often presents steep gradients at the edge, this effect has been modelled with a density pedestal n_w. This pedestal density is inserted in [N] matrix and scanned over the interval between zero and $1{:}5 \times 10^{19}$ m^{-3} . Then the difference between the experimental measurements and the corresponding line integral densities, recalculated on the basis of the reconstructed profile, are determined. The nw which minimises this difference is chosen. To quantify this error and therefore the quantity to minimise, the χ^2 parameter has been used. It can be written in the form:

$$\chi^2 = \sum_{i=1}^{n_{chords}} \left(\frac{M_i - C_i}{\sigma_i} \right)^2 \tag{15}$$

where M_i are the experimental measurements, C_i the simulated values obtained from reconstructed profile and σ_i are the uncertainties of the measurements. The quality of the results can be seen in fig.3, where a typical density profile measured by the JET Thomson scattering LIDAR [8], is compared with the reconstruction obtained by the previously described χ^2 minimisation method. This agreement has been found for all the density profiles typical of JET operation, demonstrating that the flexibility of the polynomial fit (14) is sufficient for our application

A statistical confirmation of the positive results provided by the algorithm is shown in fig.4, where the central density of our estimate is plotted versus the LIDAR experimental central value. The comparaison has been done for 123 shots, between pulse 51442 and pulse 52874, and for each times of LIDAR measurements. Figure 4. The central density estimated by the described algorithm versus the LIDAR experimental value.(The error bar of the diagnostic is typically of 10%) Many other tests to determin the reliability of the method have been performed. In particular the robustness of the iterative procedure has been checked with respect to failures of one or even two interferometric chords. In this case the code has been showen in many case to be able to detect the problem and to eliminate the unreliable signal automatically.

4. THE DERIVATION OF THE Q PROFILE

Once the magnetic topology and the density profile have been determined, the Faraday rotation measurements can be inverted to determine the profile of the poloidal field. For this goal, the poloidal field expression given by the relations (2) can be used, remembering that the derivatives of ρ with respect to R and Z depend only on the shape of the magnetic surfaces and can therefore be considered known at this stage. The quantity to be determined remains the derivative of the poloidal flux with respect to ρ which is approximated by the following polynomial:

$$\frac{\delta\Psi}{\delta\rho} = a_0\rho + a_1\rho^2 + a_2\rho^3 \qquad (16)$$

This expression is then inserted in the integrals (1), which give the Faraday rotation for the various chords, obtaining in matrix notation a relation of the type [C][a] = [ΔΓ]. Again [C] is the matrix to be inverted in order to find the coefficients [a] from the measurements [ΔΓ]. The main problem encountered in applying this method was due to the inaccuracies of the magnetic topology in the core, resulting from the uncertainty in the magnetic axis position. To overcome this difficulty, the use of a recursive procedure was again necessary. The best method found consists in varying the position of the magnetic axis in a reasonable range around a first estimate obtained by assuming $\alpha = 2$ in eq.(4). In the set of optimised shear discharges investigated, a range of 10 cm around the first estimate was found to be wide enough to cover the region in which the magnetic axis was effectively located. For each value of the magnetic axis position the magnetic surfaces in the core are recalculated and the Faraday rotation measurements are inverted in the new reference topology. The magnetic axis position, which provides the best approximation of the polarimetric measurements in the χ^2 minimisation sense, is finally chosen. At this point, the achieved reconstruction of the poloidal field, in the reference geometry of the previously determined magnetic topology, is equivalent to knowing which is the value of the poloidal field to attribute to each flux surface. Since the toroidal field is also known, the q value of each magnetic surface can be calculate on the basis of the definition expressed in equation (2). An example of a reconstructed q profile is shown in fig.5 for an optimised shear discharge and compared with result of the equilibrium code EFIT. The agreement is acceptable particularly as far as the estimate of the qmin is concerned. An extensive test campaign on 56 reconstructions relative to 31 JET discharges has shown that the results of the previously described procedure are in good agreement with EFIT reconstructions. The algorithm has recognised the nature of the profile (monotonic or reversed) in 82% of the cases. In order to obtain a significant comparing between EFIT results and reconstructions, the equilibria with EFIT have been calculated including the polarimetric measurements. In 80% of the discharges with reverse q profiles the differences between the qmin values obtained by the presented algorithm and by EFIT are within § 10% and this precision is considered sufficient for plasma control. In particular the statistics indicate for the difference a distribution with an average of 5% and a standard deviation of 5:59% as is illustrated in figure

6. On the other hand, the discrepancy between our estimate of the position of qmin and EFIT results is normally more pronunced but this effect is principally due to the uncertainty in the position of the magnetic axis. The difference in the position of qmin remains typically below 15cm. qmin reconstruction

The effects of the errors in the magnetic axis position are illustrated in fig. 7, where the difference between each q profile is due only to the different choice of the magnetic axis position. It can be noted that the magnetic axis position has a big effect on q0 but not on the qmin value. In any case, the choice of the magnetic axis position is the crucial problem of the code. The χ^2 minimisation technique, previously described, is the method adopted to define this quantity. This procedure allows typically to converge on the profile closest to the EFIT estimate as shown in fig.8.

5. OVERVIEW AND IMPLEMENTATION OF THE CODE

An overview of the final version of the code is given in fig.5, including also the measurements required at each main step of the procedure. To summarise, the necessary inputs, provided by JET real time acquisition system, are:

1) the co-ordinates of the four LCFS extreme points (top, bottom, inner and outer)

2) the co-ordinates of the intersections between the viewing chords and the LCFS

3) the values of the poloidal field in the positions defined in 1) and 2)

4) the seven interferometric and polarimetric measurements

5) the Z co-ordinate of the magnetic axis and a first estimate of its radial position

6) the toroidal field at R = 2.96 m

Data in points 1-3 derive from the magnetic measurements with some interpolation [6].

The code was implemented in C^{++} in order to match the constraints of JET real time control system, whose requirement is a reconstruction of the q profile every 50 ms at least. If the position of the magnetic axis is given as input to the code, and therefore the iteration to scan the magnetic axis position is not necessary, the computing time is about 2.5 ms on a 700MHz PC. Since a reliable estimate of the magnetic axis position is not available yet, the complete version of the code, including the scan of this parameter, had to be provided for. A careful analysis of the code has established that the most demanding operation, in terms of computational time, is the determination of the intersections between the magnetic surfaces and the viewing chords. Indeed, when the position of the magnetic axis is changed, the magnetic topology has to be modified accordingly and therefore the co-ordinates of these points have to be recalculated at every iteration. Since it is possible to express both the magnetic surfaces and the viewing chords in mathematical form, the problem of finding the intersections is equivalent to the one of determining the nulls of a

function. The adoption of the Newton-Rapson method to solve this problem and a global optimisation of the code have allowed running the complete version of the code, including the scan of the magnetic axis position, in about 20 ms. This is considered satisfactory for the present applications. Although minor adjustments to the implementation may lead to some improvements, only a better estimate of the magnetic axis position is expected to significantly reduce computing time.

The good results obtained testing these algorithms with data of previous experimental campaigns have motivated the optimisation of the code for actual real time applications. In this perspective, the program has been implemented in the JET real time system.

6. CONCLUSIONS AND FUTURE DEVELOPMENTS

To summarise, it can be stated that the devised method properly reconstructs the density and q safety factor profiles, with a time resolution and accurancy adeguate for the real time requirements of JET. Indeed, if the measurements are of acceptable quality, the density profile approximates the LIDAR measurements within § 10% and the q profile is inside an error bar of § 10%, with respect to EFIT, in almost 80% of the shots (in the optimised shear class of analysed equilibria). Future developments include plans for an extensive test campaign of the method on different classes of equilibria. Some details of the procedure will have to be adjusted for each single class but preliminary evidence seems to indicate that the approach is valid for almost all major JET discharges. The roubustness showning by the code for the determination of the density profile could therefore be used in the future to help detecting the problems posed sometimes by the fringe jumps of the interferometer. One very important topic, as shown in section 4, is the determination of the magnetic axis position. If this piece of information were available it would be possible to avoid one long iteration and the computation time would be significantly reduced. Several alternatives have already been tried to determine this parameter in real time, mainly interpolating in various ways the central chords of the polarimeter, but no acceptable solution has been found. Therefore, in the future a set of neural networks will be developed and tested in order to solve this problem in a real time compatible way.

REFERENCE

[1] C Gomerzano, JET Team

[2] M Bell et al., plasma Phys. and Control. Fusion, **41** (1999) A719

[3] E J Strait et al., Phys. Rev. Lett., **75** (1995) 4421

[4] A Becoulet et al., 28th Conference on Controlled Fusion & Plasma Physics, Madeira, June 2001

[5] J P Christiansen, Integrated Analysis of Data from JET Journal of Computational Physics **73**, 85-106 (1987)

[6] Riferimento XLOC

[7] G.H. Golub , C.F. Van Loan,Matrix Computations, The Johns Hopkins University Press, 1983.

[8] H Saltzmann et al., Nuclear Fusion **27**, 1925 (1987)

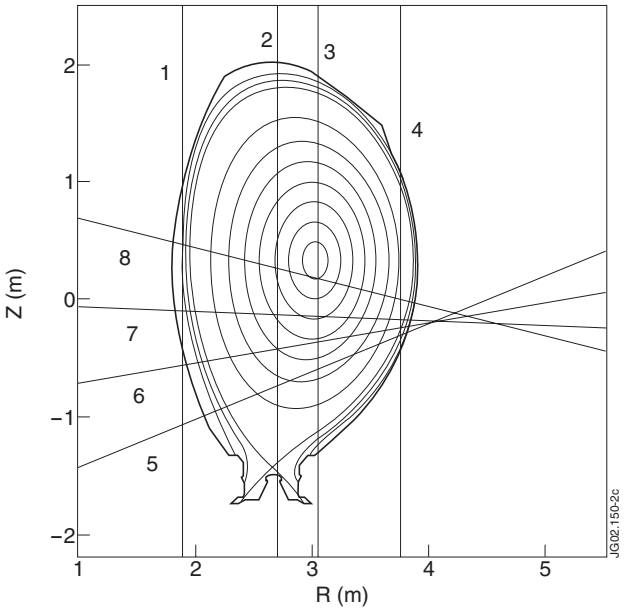

Figure.1: Interferomer-polarimeter lines of sight.

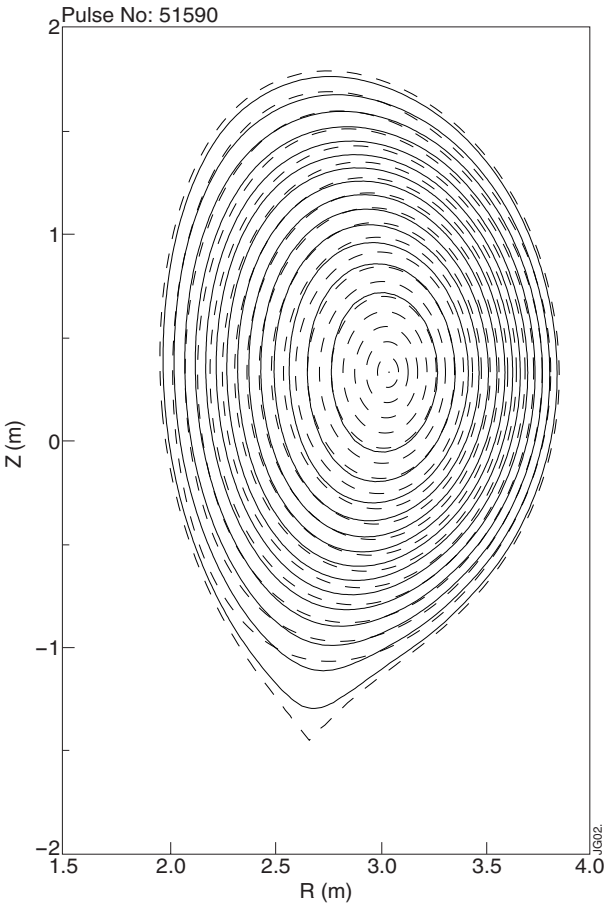

Figure.2: Comparison of EFIT magnetic topology with the one obtained by the described method.

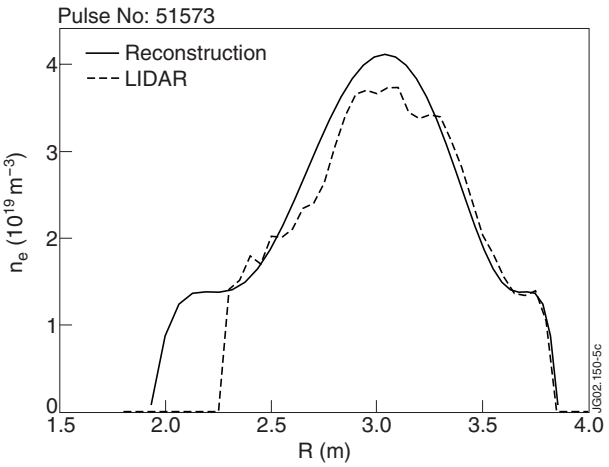

Figure.3: Comparison of LIDAR density profile with the density profile obtained by the inversion technique.

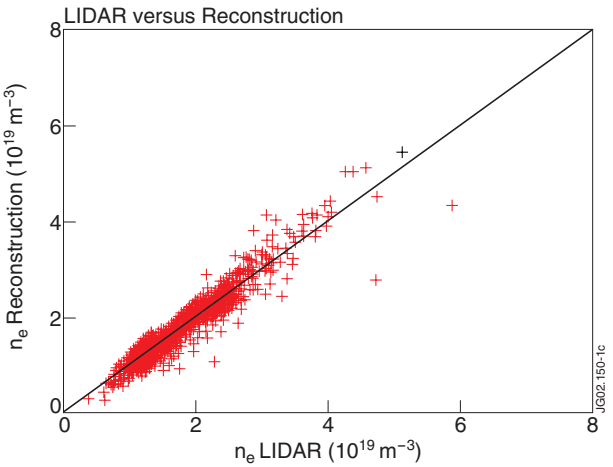

Figure.4: The central density estimated by the described algorithm versus the LIDAR experimental value.(The error bar of the diagnostic is typically of 10%).

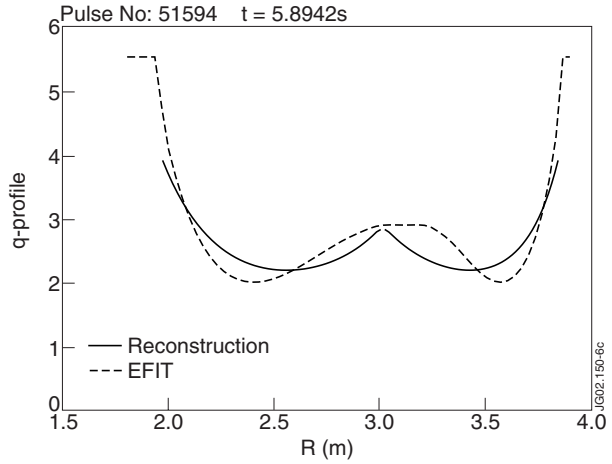

Figure.5: Comparison of our estimate of the q profile with EFIT reconstruction.

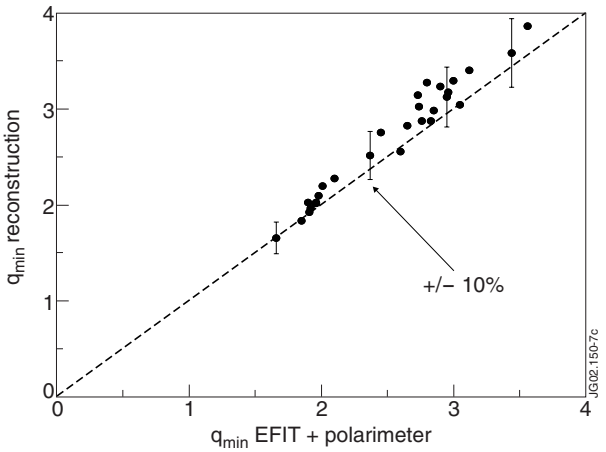

Figure.6: q_{min} EFIT vs qmin reconstruction scaling.

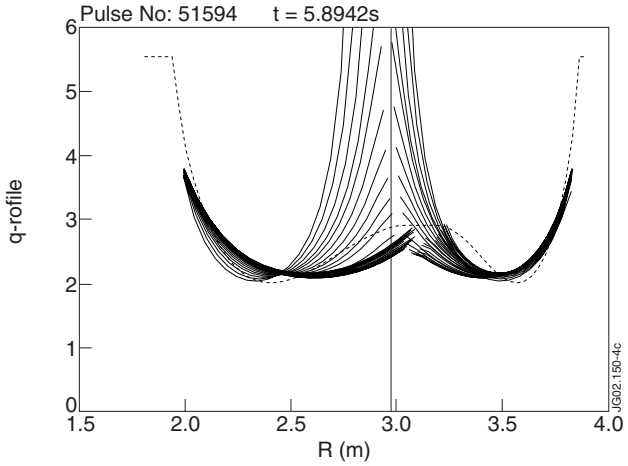

Figure.7: Magnetic axis position effect on q profile.

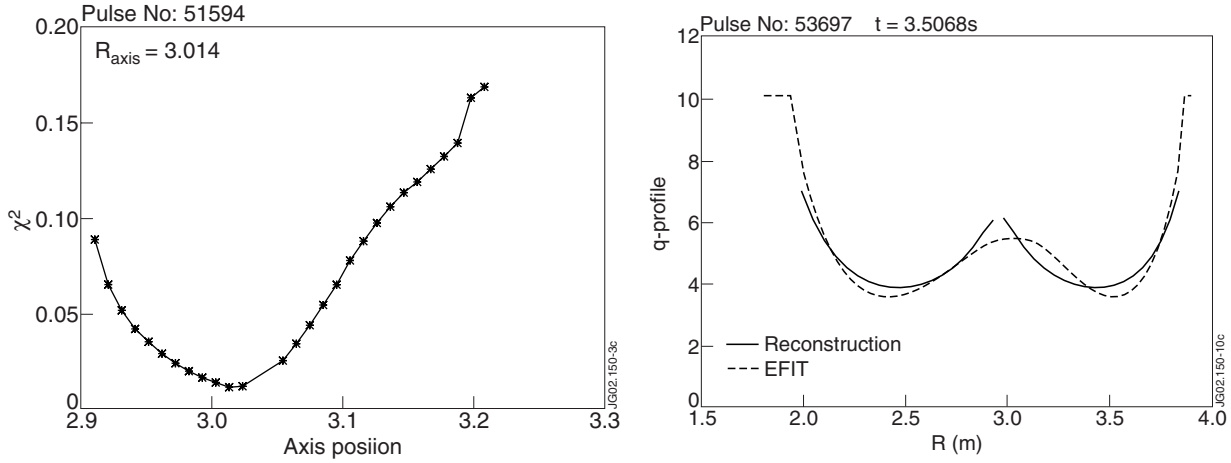

Figure.8: χ^2 minimisation method applied to the q profile reconstruction algorithm.

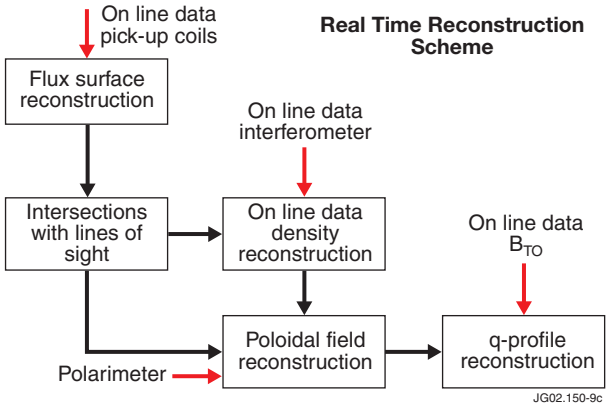

Figure.9: Block diagram of the algorithms for the reconstruction of the density and q profiles.